



# *PhysioCell* — a Novel, Bio-relevant Dissolution Apparatus: Hydrodynamic Conditions and Factors Influencing the Dissolution Dynamics

Marcela Staniszewska<sup>1</sup> · Michał Romański<sup>2</sup> · Justyna Dobosz<sup>1</sup> · Bartosz Kołodziej<sup>1</sup> · Uladzimir Lipski<sup>1</sup> · Grzegorz Garbacz<sup>1</sup> · Dorota Danielak<sup>2</sup>

Received: 13 September 2022 / Accepted: 18 December 2022

© The Author(s), under exclusive licence to American Association of Pharmaceutical Scientists 2023, corrected publication 2023

## Abstract

The physiologically relevant dissolution apparatuses simulate various aspects of gastrointestinal physiology and help to understand and predict the *in vivo* behavior of an oral dosage form. In this paper, we present and characterize for the first time a novel bio-relevant dissolution apparatus — *PhysioCell*. We evaluated the impact of several factors on the hydrodynamic conditions in the key vessel of the apparatus — the StressCell. We observed that the medium flow rate, but not the glass beads' size or amount, significantly influenced the dissolution rate. The relationship was disproportional: the increase in the flow rate from 4.6 to 9.0 mL/min reduced the dissolution time of 85% ( $T_{85}$ ) of the NaCl tablet by 46%, but from 134 to 300 mL/min decreased the  $T_{85}$  only by 24%. At the same time, the contractions of the StressCell's elastic walls promoted the content mixing and enhanced the dissolution rate of the paracetamol tablets: even very rare mixing contractions (1 per 10 min) decreased the  $T_{85}$  over twofold for the flow rate of 8 mL/min. In conclusion, the hydrodynamic conditions in the StressCell affect the dissolution of solid dosage forms and the understanding of these effects is crucial for modeling physiologically-based test conditions in the novel apparatus. Combinations of the unique *PhysioCell* features — adjustable medium flow, temperature control, controllable pH gradients and predefined mechanical agitation — can create a set of dissolution test scenarios for characterization of oral dosage forms and, in the future, making the *in vitro-in vivo* predictions.

**Keywords** Bio-relevant dissolution testing · Flow-through cell · Hydrodynamics · Mechanical agitation · Simulation of gastrointestinal passage

## Introduction

Dissolution testing is a well-established practice of evaluating the biopharmaceutical properties of oral dosage forms. Since pharmacopoeias of different countries have thoroughly normalized the dissolution methods, they are recognized as reliable worldwide. Also, quality control relies

on the results obtained by compendial methods. However, these standard approaches have limited power to accurately predict *in vivo* drug dissolution in some cases [1–3]. The possible failure in predicting *in vivo* drug dissolution most probably results from the discrepancies between the experimental setup and the conditions along the gastrointestinal (GI) tract. First, the medium volume differs from the values recorded *in vivo* [4]. It may be of great importance for poorly soluble drugs. Second, the temperature of the gastric content after fasting intake of a dosage form is not instantaneously equal to 37°C as in pharmacopoeial dissolution tests. It gradually increases from the room temperature of a co-administered glass of water to the body temperature [5]. This temperature gradient was proved to significantly impact the disintegration of hard gelatin capsules [6]. Third, the pharmacopoeial media for dissolution studies, such as phosphate buffer, do not adequately reflect the composition of GI fluids [7]. Moreover, the compendial apparatuses

✉ Marcela Staniszewska  
M.Staniszewska@physiolution.pl

<sup>1</sup> Physiolution Polska, 74 Pilsudskiego St., 50-020, Wrocław, Poland

<sup>2</sup> Department of Physical Pharmacy and Pharmacokinetics, Poznan University of Medical Sciences, 3 Rokietnicka St., 60-806, Poznan, Poland

do not apply mechanical stresses of physiological intensity. Garbacz et al. [8] showed that including bio-relevant conditions, such as mechanical stress, during dissolution studies allowed to predict irregular absorption profiles of extended release sodium diclofenac formulations. Also, the flow pattern present in the pharmacopoeial apparatuses, operating under standard conditions (50 and 100 rpm), does not correctly reflect GI hydrodynamics [9, 10]. Finally, the intestinal passage of the dosage form is also interrupted by spaces where gastrointestinal juice is not present, which is not considered in pharmacopoeial dissolution [4].

These factors indicate that the compendial methods may not fully assess the newly developed formulation's properties, such as susceptibility to mechanical stress or physiological fluids. Well-described phenomena, such as dose dumping caused by mechanical agitation, may result in strikingly different pharmacokinetic profiles between the test and reference products administered to the same individual. In such circumstances, the ratios of main pharmacokinetic parameters may fall outside the required 90% confidence interval, leading to the failure of the bioequivalence trial. Using non-standard dissolution tests in equipment resembling physiological conditions may partially solve this problem. Currently, several noncompendial apparatuses are available on the market [11, 12]. They include sophisticated multicompartments solutions that mimic an entire GI tract, such as TNO TIM-1 [13]. Simplified models utilize one- or two-compartments. Such devices are Advanced Gastric Simulator [14], Dynamic Gastric Model [15], Stress Tester [8], BioGIT [16], and GastroDuo [17]. A recently published excellent review summarized the developed models simulating human GI motility [18]. Also, a review by the European Network on Understanding Gastrointestinal Absorption-related Processes (UNGAP) [19] highlighted the trend of designing such advanced bio-relevant dissolution methodologies. The ultimate goal of these solutions is to find a balance between the complexity of the GI tract conditions and the simplicity of the dissolution methods.

In this paper, we characterize for the first time a novel bio-relevant dissolution apparatus — *PhysioCell*, Physiologia Polska [20]. We hypothesized that the parameters of the *PhysioCell* such as fluid flow rate, size and amount of glass beads, and frequency of the sleeve contractions affect the dissolution process. Therefore, the study aimed to describe and comprehend the impact of the hydrodynamic conditions offered by *PhysioCell* on dissolution, with or without mechanical agitation. This knowledge could be utilized to develop subsequent physiologically-based and reliable dissolution experiments, combining repeatability of the test with bio-relevant features of the apparatus.

## Materials and Methods

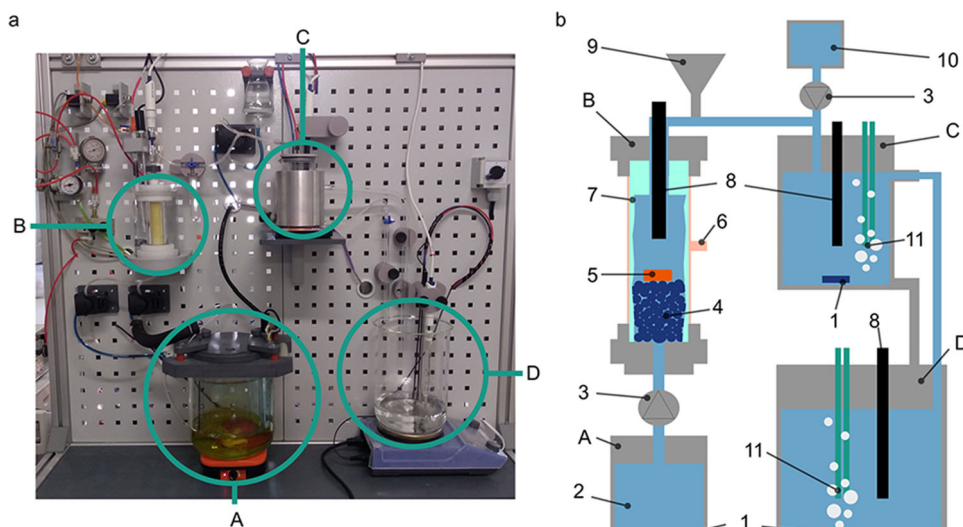
### Description of *PhysioCell* Apparatus

*PhysioCell* is a recently designed and constructed multi-compartment apparatus for noncompendial dissolution testing. Compartments of the device can imitate conditions of the GI sections: stomach, duodenum, small intestine, and the initial fragment of the large intestine, although none of the vessels is an exact replication of a human organ. *PhysioCell* can therefore simulate the dissolution of a drug throughout the GI passage, and in its individual fragments, both under fasting and fed conditions. The *PhysioCell* was designed mainly for immediate release products, such as hard capsules, soft capsules, tablets with a variety of disintegration characteristics (both fast and slow) and tablets with microenvironment modifiers (e.g., pH modifiers). For these dosage forms, the apparatus offers complex, bio-relevant dissolution tests, visual inspection by an endoscopic camera, assessment of a disintegration process, and determination of the impact of a formulation on the local pH gradients. Also, the *PhysioCell* can be a valuable tool for testing delayed release dosage forms, for example, to verify if enteric-coated units withstand the pressure waves typical for the passage through the stomach pylorus to the duodenum. The extended release formulations could be tested after further adjustment of the test protocols since the flow-through methodology might be inaccurate due to long experimental runs and small API concentrations. In this study, we focused on several immediate dosage forms and the tests with both modified and extended release formulations were outside of the scope.

The novel apparatus consists of three vessels: the *StressCell*, the *Overflow Vessel*, and the *Collection Vessel*, connected with Tygon<sup>®</sup>, silicone and PCV tubings of diameters 2–4 mm (Fig. 1). Table I summarizes the features offered by each vessel.

The *StressCell* is a double-walled flow-through cell (internal diameter 24.2 mm, height 132 mm) equipped with an elastic sleeve. The inlet of a medium is in the center, at the bottom of the *StressCell*, and the outlet is in the vessel's lid. The external *StressCell* walls are fixed, while an elastic latex sleeve serves as an inner wall. During the experiment the two walls of the *StressCell* are in close contact. The compressed air may flow between the walls, changing the inner diameter of the cell. The air pressure is controlled by a regulator and can be manually adjusted. Thus, the sleeve enables the application of a pressure of physiological range (up to 500 mbar) on a dosage form [21]. When the mixing contractions or pressure waves are applied, the compressed

**Fig. 1** PhysioCell apparatus in open-loop configuration: A — reservoir for a dissolution medium in a water bath, B — The StressCell in a water bath, C — The Overflow Vessel, D — The Collection Vessel. **a** Photographic representation of the apparatus. **b** Schematic presentation of PhysioCell: 1 — magnetic stirrers, 2 — a dissolution medium, 3 — peristaltic pumps, 4 — the bed of glass beads, 5 — a tested dosage form, 6 — compressed air inlet, 7 — the elastic sleeve, 8 — pH probes, 9 — The Expansion Tank, 10 — a neutralizing agent, 11 — gas diffusers



air fills the gap between the walls. For the mechanical stress application on a dosage form, air of desired pressure fills the gap between the walls and stretches the sleeve that finally occludes on a dosage form. The tested dosage form is placed either on a layer of glass beads or in the middle of the cell, inside the sleeve, and squeezed at predefined time points. A mechanistic approach of incorporating mechanical agitation was valuable for predicting the susceptibility of HPMC matrices to mechanical agitation [1]. Also, a method of mixing the content of the flow-through cell, coupled with the cell of special design and the system containing the latter, is described in patent application [20]. Briefly, at the fixed time points, compressed air is let to the *StressCell* for 1 s only. The elastic sleeve moves gently, however, it does not contact a dosage form directly. Thus the medium in

the *StressCell* is delicately mixed, but no mechanical force is exerted on a dosage form. The elastic sleeve is easily maintained and replaced typically once per ca. six months to avoid changes in its elasticity.

The peristaltic pump supplies the *StressCell* with pharmacopoeial or noncompendial media at a user-defined rate: it is able to work in a volumetric flow range from 4 to 350 mL/min. A water bath keeps the medium temperature in the *StressCell* at 37°C; however, it can be regulated by a dedicated heater. This setup allows simulating the temperature gradient that occurs when a fasting individual ingests the drug with a glass of still (non-carbonated) water at room temperature. Then, the stomach content temperature increases gradually in the range of 25–37°C. The pH-electrode built in the *StressCell* allows

**Table 1** Summary of the Features Offered by the *PhysioCell* Compartments

	The StressCell	The Overflow Vessel	The Collection Vessel
Mechanical agitation	✓	×	×
Mixing contractions	✓	×	×
Temperature gradient	✓	×	×
Variable flow rate	✓	✓	×
Neutralization	×	✓	×
pH gradients	✓	✓	✓
Volume	Ca. 20 mL	200 mL	Up to 3 L
GI section simulated	stomach, small intestine	duodenum, small intestine	small intestine, proximal colon

an in-line pH measurement. Since the main dissolution vessel of the *PhysioCell* is the *StressCell*, in the present report, we focused on a thorough characterization of this compartment.

The second vessel of the apparatus is the *Overflow Vessel*. It collects and neutralizes the medium flowing from the *StressCell*. Also, owing to the pH-electrode placed in the vessel and the *physio-Grad*<sup>®</sup> module, the *Overflow Vessel* can operate with a hydrogen carbonate buffer. Thus, performed tests can include neutralization to a constant pH and simulation of physiological pH gradients, reflecting those found in the human intestine [21, 22].

The apparatus's last and largest vessel (3 L) is the *Collection Vessel*, dedicated to accumulate an active pharmaceutical ingredient (API) under sink conditions. Ideally, the *Collection Vessel* should contain 100% of the tested dose at the end of the experiment. Like the *StressCell* and the *Overflow Vessel*, the media pH in the *Collection Vessel* can be monitored and adjusted to reflect the physiological conditions.

*PhysioCell* is built upon a set of microcontrollers, motors, switches, and sensors. Currently, predefined scenarios in Python scripts control the settings and allow customization of volumetric flow rate, timing and magnitude of the pressure events, temperature gradients, pH gradients, and frequency of mixing contractions. Dedicated software is under development to allow easier scenario modification according to the user's requirements.

## Preparation of the Dissolution Experiments

For the dissolution experiments, firstly the *StressCell* was assembled. The elastic sleeve mounted inside the *StressCell* was semi-transparent which hindered the observations of the flow pattern. Therefore, in the first step of the preparation, the elastic sleeve was temporarily removed from the cell when a visual assessment was necessary. Then the cell inlet was plugged with a 6 mm bead, which prevented the medium and glass beads from falling back into the vessel's feed line. The bed of glass beads was piled on a holder was mounted and a dosage form was placed on. Next, the upper lid of the cell and the tubing were installed. The *StressCell* was fixed into the *PhysioCell* apparatus. In the experiments with *NaCl* and *Strepsils*<sup>®</sup>, the cell outlet was equipped with a tube, and the samples for determination of the analyte concentration were collected as subsequent fractions. These experiments were performed in an open-loop configuration. Experiments with paracetamol were performed in a closed-loop setting with the *StressCell* and medium reservoir; the latter was also a sampling site. Also, in the experiments with paracetamol, the water baths of

the *StressCell* and the medium reservoir were warmed up to 37°C. Finally, the experiments were launched with a predefined test scenario from the command line, since the work of the apparatus is automated. *PhysioCell* allows both manual and automated sampling; in the described experiments, samples with *NaCl* and *Strepsils*<sup>®</sup> were withdrawn manually, while paracetamol samples were taken automatically.

## Materials

*Strepsils*<sup>®</sup> lozenges, (Reckitt Benckiser Poland, Nowy Dwór Mazowiecki, Poland), containing flurbiprofen 8.75 mg, *Paracetamol Synoptis* 500 mg, (Synoptis Pharma, Warszawa, Poland) and kalium hypermanganicum (KMnO<sub>4</sub>) tablets (FSP "GALENA", Wrocław, Poland) were purchased from a local pharmacy. Paracetamol, USP Powder, was purchased from Sigma Aldrich. Sodium chloride, 99.9%, was purchased from VWR Chemicals. Potassium dihydrogenphosphate (Reag. Ph. Eur, 99.7%) and sodium hydroxide pellets (Reag. Ph. Eur., 99.1%) were purchased from VWR Chemicals. Bromophenol blue (ACS, Reag. Ph. Eur.) was purchased from Merck Millipore. Ultra-pure water from the purification system - ULTRA, Hydrolab was used.

The goals of the experiments drove the choice of the substances and dosage forms used for *StressCell* characterization: (1) to quickly and reliably assess the medium flow pattern in the vessel; (2) to determine the influence of hydrodynamic conditions on a dissolution profile without application of mechanical stress; (3) to examine how mechanical agitation impacts the dissolution of a typical immediate release oral dosage form.

For the first task, a solution of potassium permanganate (KMnO<sub>4</sub>) (Kalium Hypermanganicum (GALENA, Wrocław, Poland)) was chosen. Its intense color allowed qualitative assessment of the course of the liquid stream inside the *StressCell*.

For the second task, additional criteria had been proposed. The aim was to check the uniformity of dissolution process in the *PhysioCell* apparatus and ascertain that the results are not hindered by, for example, the variable size distribution of the particles formed after the dosage form disintegration. Also, the object used for the research should be repeatable in terms of quantitative and qualitative composition, size, and release kinetics. These conditions are met by the medicinal products, as it is required for authorizing them for the markets. Thus, *Strepsils*<sup>®</sup> Intensive (Reckitt Benckiser S.A., Poland) hard lozenges with 8.75 mg flurbiprofen were chosen. The lozenge's advantage is homogeneous API distribution

within. The second substance selected was sodium chloride. *NaCl* was chosen due to its high solubility and ease of measurement with chloride ion-selective electrode. Also, it enabled observations of the dissolution process unaffected by diffusion and dissolution of other excipients. The *NaCl* tablets were manufactured in-house. First, *NaCl* crystals were micronized with a hand mortar to increase their ability to flow during tableting. Next, tablets of 13 mm diameter were hand-pressed using punch tablet press.

For the third task, *Paracetamol Synoptis* 500 mg was selected — as it is a popular, rapidly disintegrating tablet (disintegration time ca. 1 min). As previously stated, this formulation's choice was dictated by a good solubility of the API and expected repeatability of the dissolution process required for the marketed formulations.

### Dissolution Media and Analytical Methods

Dissolution medium for *NaCl* consisted of freshly prepared ultra-pure water only. Flurbiprofen dissolution medium was 50 mM phosphate buffer, pH 6.8. Both dissolution media were at room temperature (21–22°C). The dissolution medium for paracetamol was SGF (Simulated Gastric Fluid), which consisted of 2 g/L *NaCl* with pH adjusted to 1.8 with HCl.

The concentration of chloride ions was determined through offline measurement with  $\text{Cl}^-$  selective electrode *perfectION*<sup>TM</sup> (Mettler Toledo) coupled with the *SevenMulti* meter. Samples were derived as subsequent fractions of a dissolution medium collected at the outlet of the *StressCell*. A fresh stock solution of *NaCl* dissolved in ultra-pure water was prepared daily. Before dissolution experiments, we validated the method and confirmed its linearity and precision within the concentration range of  $5.85 \cdot 10^{-3}$  to 15.1 mg/mL.

UV-Vis spectroscopy was utilized to determine flurbiprofen concentration in dissolution samples. The samples were collected as fractions of the dissolution medium flowing out of the *StressCell*. The absorbance of samples and standards were measured offline at 246 nm with UV-Vis Agilent 8453 spectrophotometer and quartz cuvette with a 10 mm optical path (Hellma Analytics). Selectivity of this method was assessed by comparison of dissolution medium spectrum with spectrum of a standard solution of *Strepsils*<sup>®</sup> lozenge dissolved in the medium. Since the working standard of flurbiprofen was unavailable, ten tablets were weighed, and the average lozenge mass was assumed to contain 8.75 mg of the API, as labeled. In the dissolution tests, the API content was assumed to be proportional to the mass of a lozenge.

The concentration of paracetamol was determined spectrophotometrically, similarly to flurbiprofen. Since the

experiment was performed in a closed-loop configuration, samples were withdrawn automatically from the medium reservoir, through a PE cannula filter (1  $\mu\text{m}$ ) and transferred to the spectrophotometer for online analysis. The absorbance was measured at 280 nm in a 1 mm optical path of quartz cuvettes (Hellma Analytics). The method was validated in terms of linearity and precision within the API concentration range of 0.10 to 0.60 mg/mL.

### Characterization of StressCell Hydrodynamic Conditions

In order to characterize the hydrodynamic conditions of the vessel, we performed the following tests: visual inspection of medium flow, the influence of the glass beads size, the influence of the glass bead layer thickness, and dissolution of two solid dosage forms under selected medium flow and glass beads. Final experiments focused on evaluating the influence of elastic sleeve contractions on the mixing of the *StressCell* content and API dissolution.

#### Media Flow Visualization

As previously mentioned, the initial visual assessment involved a  $\text{KMnO}_4$  solution. Before the experiment, the cell was packed with a layer of medium glass beads (2 mm diameter) and filled up with tap water. The vessel's feed line was connected to a reservoir of  $\text{KMnO}_4$  solution (concentration circa 0.1 mg/mL), and the medium was pumped with a predefined rate of 8, 12, and 50 mL/min.

#### The Glass Bead Layer

In order to examine the impact of glass bead diameter on the dissolution kinetics, we measured the dissolution of *NaCl* tablets at a constant water flow rate of 10 mL/min. Three different sizes of glass beads were used: small (0.35 mm diameter), medium (2 mm diameter), and large (mixed sizes in the range 2.85–4.85 mm). The thickness of the glass beads layer was 60 mm. Also, an experiment was conducted using an in-house constructed metal holder instead of glass beads. To investigate the impact of bed thickness on dissolution, we performed experiments with medium-sized beads, 10 mL/min medium flow rate, and with the layer heights 20, 40, 60, and 80 mm.

#### Medium Flow Rate and Direction

We investigated the impact of the medium flow rate and flow direction on the dissolution of solid dosage forms for *Strepsils*<sup>®</sup> lozenges and *NaCl* tablets. A tested dosage

form was placed on the layer of medium size glass beads. The thickness of the bed was 40 mm for *NaCl* tablets and 20 mm for *Strepsils*<sup>®</sup>. The time of complete dissolution was assessed visually. Additional tests were carried out with a reversed flow downwards the *StressCell*. Due to the construction of the system, the medium had to be pumped out at the outlet of the cell and not into the vessel as in the original configuration. The inlet of the cell was not secured with a larger glass bead, but the dosage form was placed on a metal holder at the height of 40 mm (*NaCl*). The flow rates in this part of the experiment corresponded to the values applied in tests with an upward flow: 10 mL/min and 30 mL/min.

### Contraction-Induced Content Mixing

We designed two experiments to determine how the contractions of the sleeve influence the mixing of the *StressCell* contents. First, we filled the cell with 5 mM phosphate buffer pH 4.0 with bromophenol blue and switched the supply medium to a buffer of pH 10.0. The elastic sleeve was not mounted in the cell. That way, we could record with a web camera how the flow pattern behaves during the neutralization at various flow rates: 4, 8, 12 mL/min. Next, we used the same media and flow rates but with the sleeve mounted inside the vessel. The tests were carried out without contractions of the sleeve and with contractions at a 1 per minute rate. During the test, we recorded how the pH inside the *StressCell* changed over time with 5 s intervals.

To assess the impact of various mixing conditions of the *StressCell* content, we performed dissolution tests of rapid-disintegrating tablets containing 500 mg paracetamol. Tablets were placed on a 40 mm layer of medium size glass beads and the cell was perfused with SGF at the flow rate of 4, 8, and 12 mL/min. The test scenario included mixing the cell's content with contractions of the elastic sleeve. The contractions were mild enough not to impact the integrity of the dosage form and were applied with various frequencies: 1 per 1, 5, 10 min, and without any contractions.

### Data Analysis and Visualization

The data used for the determination of dissolution rate were the fraction of the drug dissolved ( $D$ , [%]). Then, derivatives of the amount of the drug dissolved with respect to time were calculated. Numerical determination of function derivatives was performed with an open license *LabPlot* software, version 2.7, available from <https://labplot.kde.org/>. LibreOffice Impress software (version 6.4.7.2., The Document Foundation, Germany) and LabPlot were utilized for data visualization. Time of dissolution of 85% of the dose ( $T_{85}$ ) was linearly interpolated.

## Results

### Hydrodynamic Characterization of the *StressCell*

#### Medium Flow Pattern Inside the *StressCell*

During the experiment with  $\text{KMnO}_4$ , we observed a flow pattern symmetrical about the *StressCell* axis at flow rates of 8, 12, and 50 mL/min (Fig. 2). Interestingly, the system produced a parabolic profile of medium at the slowest flow rate. The flow profile flattened and blurred with the increase in the flow rate; however, no notable fluctuations were observed.

#### Sizes of Glass Beads

We observed that the smallest beads formed a loose bed during the experiment. A *NaCl* tablet collapsed into the bead layer, and only its top side was visible. This unusual behavior was reflected in a dissolution profile and its derivative. Under these conditions, the dissolution was the quickest. In the case of other sizes of beads, a tablet remained on top of the bead layer during the whole dissolution process. The dissolution curves for medium and large beads were similar (Fig. 3a). However, derivatives of these functions have a different course from 15 to 17 min, corresponding to the tablets' dissolution time (Fig. 3b). Also, the derivative for medium beads reached zero faster than for large beads, suggesting an easier washing out of the dissolved material from the *StressCell*.

#### Thickness of the Glass Beads Layer

Obtained dissolution profiles (Fig. 3c), their derivatives (Fig. 3d), and the observed time of complete dissolution (around 17 min) are very alike. However, we noticed that increase and decrease of derivatives reflects the order of thicknesses of the glass beads layer, with the latest curve for 20 mm beads, then 40 mm and 60 mm. When a tablet was placed on an 80 mm bead layer, the dissolution was the quickest.

#### Dissolution at Various Flow Rates

This experiment's results clearly show that the dissolution rate depends nonlinearly on the medium flow rate. Table II includes complete dissolution time of *NaCl* tablets assessed visually, and the  $T_{85}$  estimated by linear interpolation of two adjacent points. Figure 4 presents summarized dissolution data. Detailed graphs depicting dissolution with all the tested flow rates are included in the [Electronic Supplementary Files](#). For the profiles recorded at low flow rates, 4.6–42 mL/min, even a slight increase in the flow

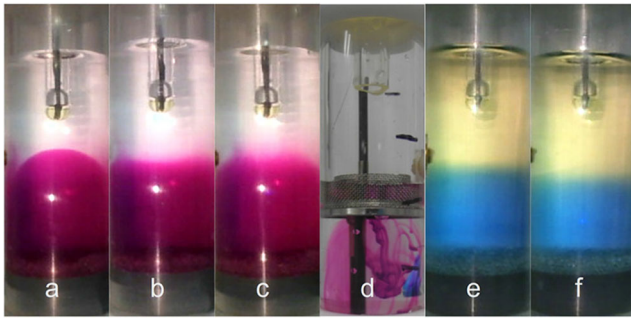
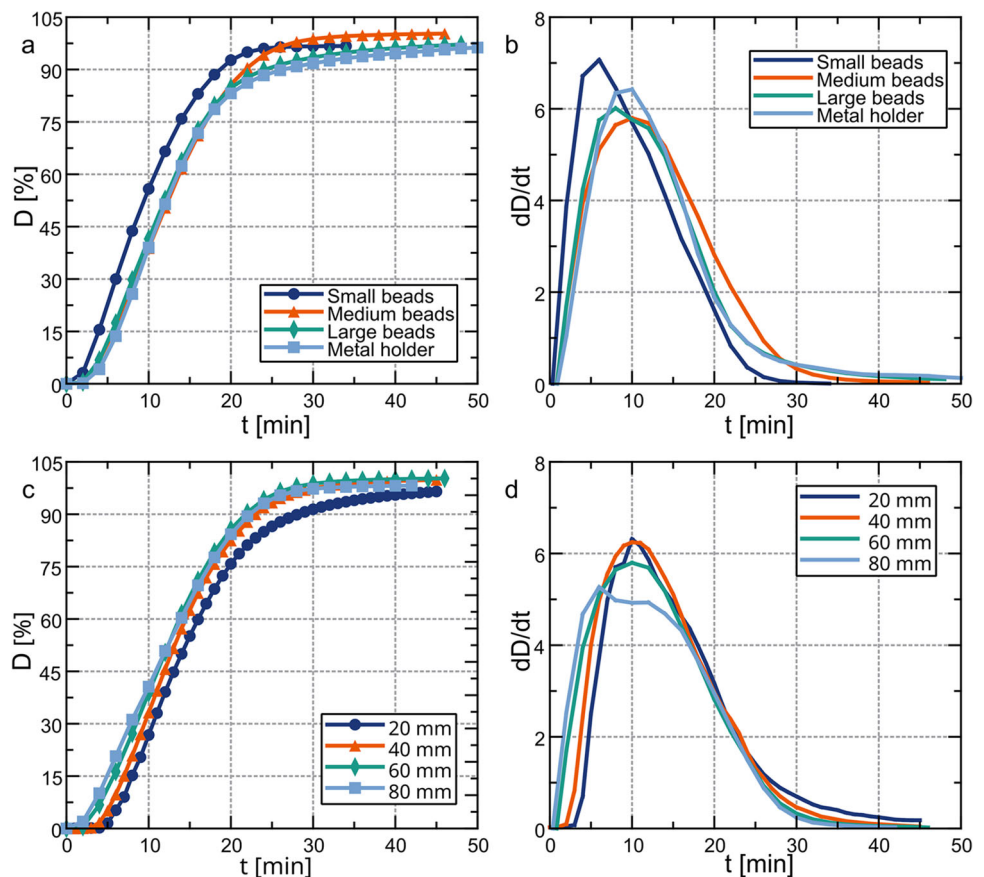


**Fig. 2** Flow patterns in the StressCell: **a**  $\text{KMnO}_4$  with flow rate of 8 mL/min, **b**  $\text{KMnO}_4$  with flow rate of 12 mL/min, **c**  $\text{KMnO}_4$  with flow rate of 50 mL/min, **d**  $\text{KMnO}_4$  tablet placed on a holder, **e** bromophenol blue visualizing the pH gradient of phosphate buffer with flow rate of 4 mL/min and **f** bromophenol blue visualizing the pH gradient of phosphate buffer with flow rate of 8 mL/min

rate profoundly changed the dissolution curve and the  $T_{85}$  of NaCl tablets decreased nearly 4-fold: from 38 min to 10 min. When the flow rate increased up to 134 mL/min, the profiles became similar and the  $T_{85}$  decreased from 10 to 7 min. Finally, the flow rates from 188 to 300 mL/min caused only minor changes in dissolution rates and only 1 min shorter  $T_{85}$ .

**Fig. 3** The influence of glass beads size (Graphs **a** and **b**) and the thickness of glass beads layer (Graphs **c** and **d**) on the NaCl tablets dissolution



In the analogous experiments performed with the *Strepsils*<sup>®</sup>, we observed different behavior (Table III). The dissolution curves for the flow rates between 4.6 and 44 mL/min have a time shift; however, their slope is comparable (Fig. 4c). Similar dissolution profiles course was obtained for the flow rates 44 and 81 mL/min, but the plateau phase was reached faster for higher flows.

An in-depth analysis of derivatives of dissolution profiles shows their smooth course for flow rates up to 22 mL/min in contrast to rugged functions for flows 42 mL/min and higher. It may result from either higher homogeneity of the cell's content, concentration averaging by long sampling times or greater accuracy of manual sampling at low flow rates. It is also characteristic, that derivatives are right-skewed, with rapid increase and almost exponential decrease.

Another observation is a considerable difference between the visually assessed dissolution time and the one obtained from curve analysis ( $T_{85}$ ). For example, at the 4.6 mL/min flow rate, the observed time was only 1.5 min shorter than for the higher flow rate, while the  $T_{85}$  was over two times longer than for flow of 9 mL/min. This reversed tendency is not met for faster flow rates.

Figure 5 presents dissolution time assessed by visual observation *versus* the medium flow. An exponential

**Table II** Dissolution Time of NaCl Tablets Under Various Flow Rates

Flow rate [mL/min]	4.6	9.0	22	42	63	86	134	188	253	300
Dissolution time <sup>a</sup> [min]	16.0	17.5	16.0	14.0	13.0	13.0	11.5	10.0	9.0	9.0
T <sub>85</sub> <sup>b</sup> [min]	38.4	20.9	13.9	10.2	8.9	9.6	7.4	5.9	6.1	5.6

<sup>a</sup>Visually assessed complete dissolution time.

<sup>b</sup>T<sub>85</sub> — 85% drug product dissolution time.

function described the behavior of NaCl tablets well when the slowest flow was rejected ( $R^2 = 0.98$ ). For *Strepsils*<sup>®</sup> the amount of data was too little to unquestionably describe it with similar function. It can be anticipated that at high flow rates, above 200 mL/min, the dissolution time reaches a minimum value. Experimental dissolution time at 4.6 mL/min was much shorter than estimated by the exponential function (16 vs. 20 min).

### The Influence of the Flow Direction

To further investigate effects accompanying the dissolution at the lowest medium flow rates, we conducted experiments with a medium flowing in the opposite direction, downwards the *StressCell*. This change increased the NaCl

tablet dissolution rate, as seen in Fig. 6. The effect was also observed at the faster medium flow rate (27.3 and 27.5 mL/min); however, it was less pronounced. The complete dissolution time confirmed the observations from the slopes of the dissolution curves: the process was the fastest in the medium flowing at a rate of 27.5 mL/min down the cell (15 min) and the slowest at 8.4 mL/min upwards (17–18 min). Additionally, we observed faster elution of the dissolved material from the cell when the medium flowed from the top to the bottom.

### Mixing of the Content of the StressCell

The flow pattern during the pH gradient formation in the *StressCell* was uniform and reproducible under a flow rate

**Fig. 4** Influence of various flow rates on the dissolution of NaCl tablets (Graphs **a** and **b**) and *Strepsils*<sup>®</sup> lozenges (Graphs **c** and **d**)

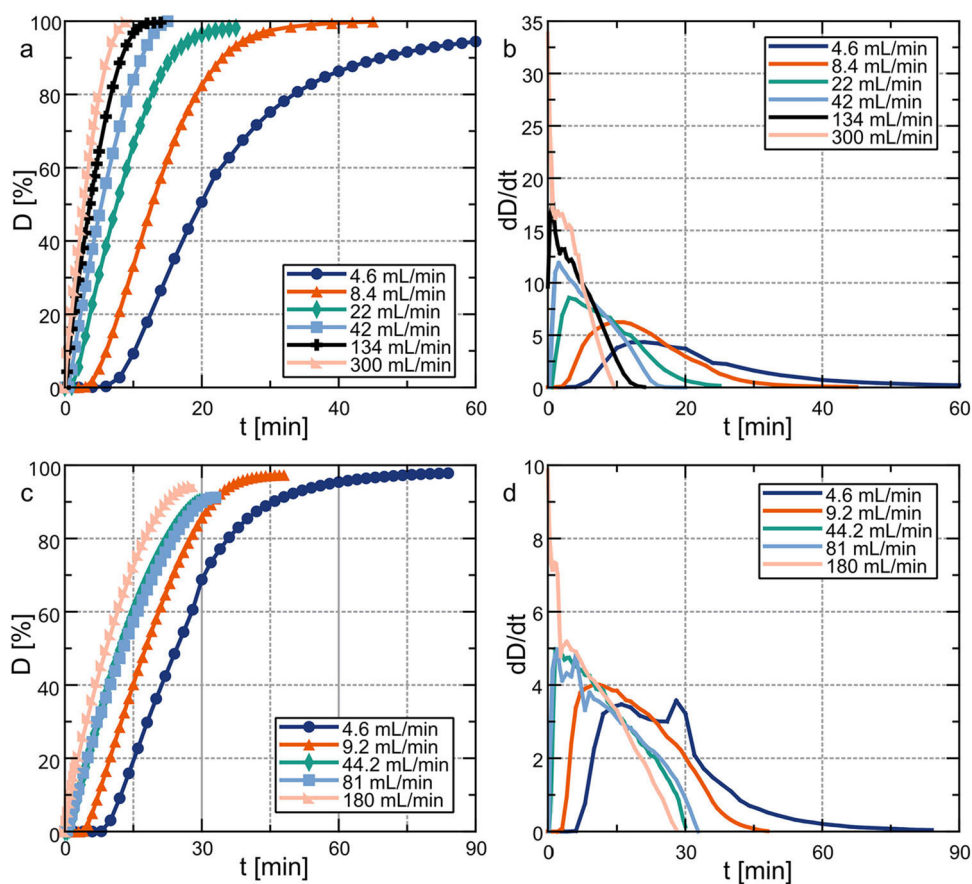




**Table III** Dissolution Time of 85% of *Strepsils*<sup>®</sup> Lozenges Under Various Flow Rates

Flow rate [mL/min]	4.6	9.2	44.2	81	180
$T_{85}$ [min]	39.8	29.7	25.1	26.4	19.7

of 4 and 8 mL/min, as seen in Fig. 2. It resembled conditions observed during experiments with  $\text{KMnO}_4$  and the media flow 12 mL/min. The piston-like flow of the medium during the experiment with no contractions of the sleeve caused a rapid change of pH in the StressCell (Fig. 7 a-c). When we imposed the sleeve contractions, the pH gradient was strikingly different. The pH started to increase sooner, but the process was more variable and occurred at a slower rate. Moreover, only when the flow was the slowest we observed contraction-induced pH fluctuations in the nearest vicinity of the electrode. These observations confirm that the mechanical agitation significantly influenced the mixing process of the medium inside the *StressCell*.

Finally, the experiments with paracetamol tablets allowed us to determine the influence of the flow rate and contractions on the solid dosage form dissolution. We performed experiments with various frequencies of contractions of the elastic sleeve — one per minute, one per 5 min, one per 10 min, and without contractions — and with three flow rates: 4, 8, and 12 mL/min. Based on the obtained dissolution profiles of paracetamol (Fig. 7 d-f), we noticed that the dissolution rate increased along with the contraction frequency. The most pronounced effect was observed for the 4 mL/min flow rate. When there were no contractions, the dissolution was too slow to ascertain that all of the paracetamol dissolved within 90 min and only half of the total drug amount dissolved at the end of the experiment. For 8 mL/min the  $T_{85}$  decreased from 85 to 27 min, when the mixing contractions were introduced in a frequency of 1 per minute (Table IV). The only deviating observation is the dissolution profile under the flow of 12 mL/min and no

simultaneous contractions — it shows a faster dissolution during the first 25 min than dissolution with one contraction per 10 min. These results prove that additional mixing by elastic sleeve contractions accelerates dissolution and prevents the retention of dissolved material in the cell.

## Discussion

The present study characterizes for the first time the novel bio-relevant dissolution apparatus, *PhysioCell*, with the focus on its central component — the *StressCell*. We confirmed the hypothesis that the medium flow rate, along with the contractions of the built-in elastic sleeve, has the greatest impact on the dissolution of the tested materials. However, other tested factors, such as the thickness of the glass beads layer, have little influence on the dissolution process.

*PhysioCell* has a multicompartmental structure, but its primary dissolution chamber bears some resemblance to

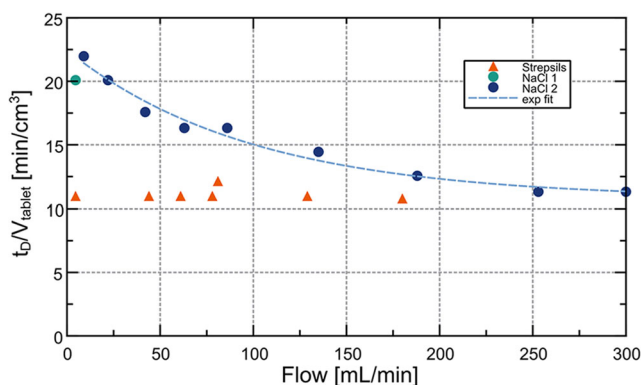


**Fig. 5** Influence of the medium flow rate on the dissolution time of NaCl tablets and *Strepsils*<sup>®</sup> lozenges. The dashed line indicates an exponential function ( $R^2=0.98$ ) fitted to the data of NaCl tablets for the flow rates of 9 mL/min and higher

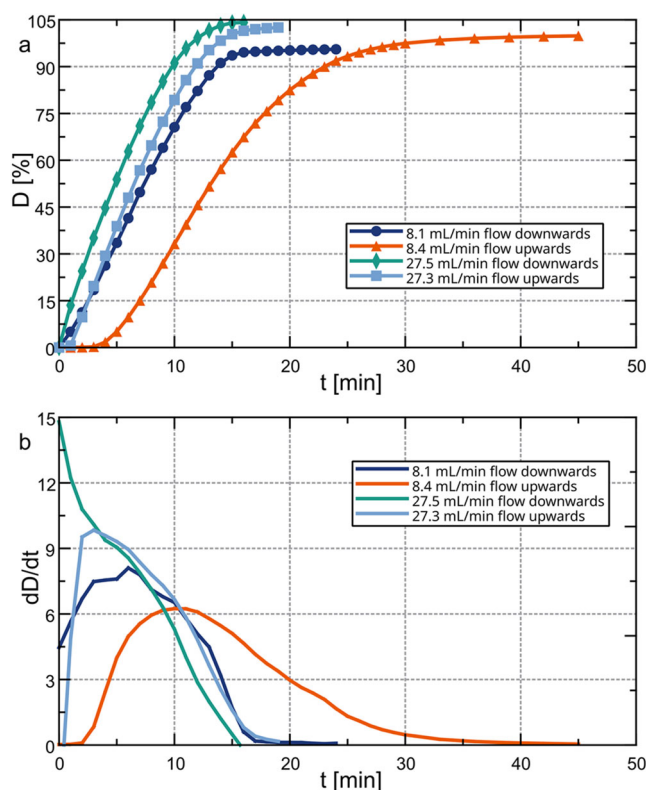


**Fig. 6** Comparison of dissolution of NaCl tablets with upward and downward flow of the medium. **a** Dissolution profiles, **b** derivatives of the dissolution profiles

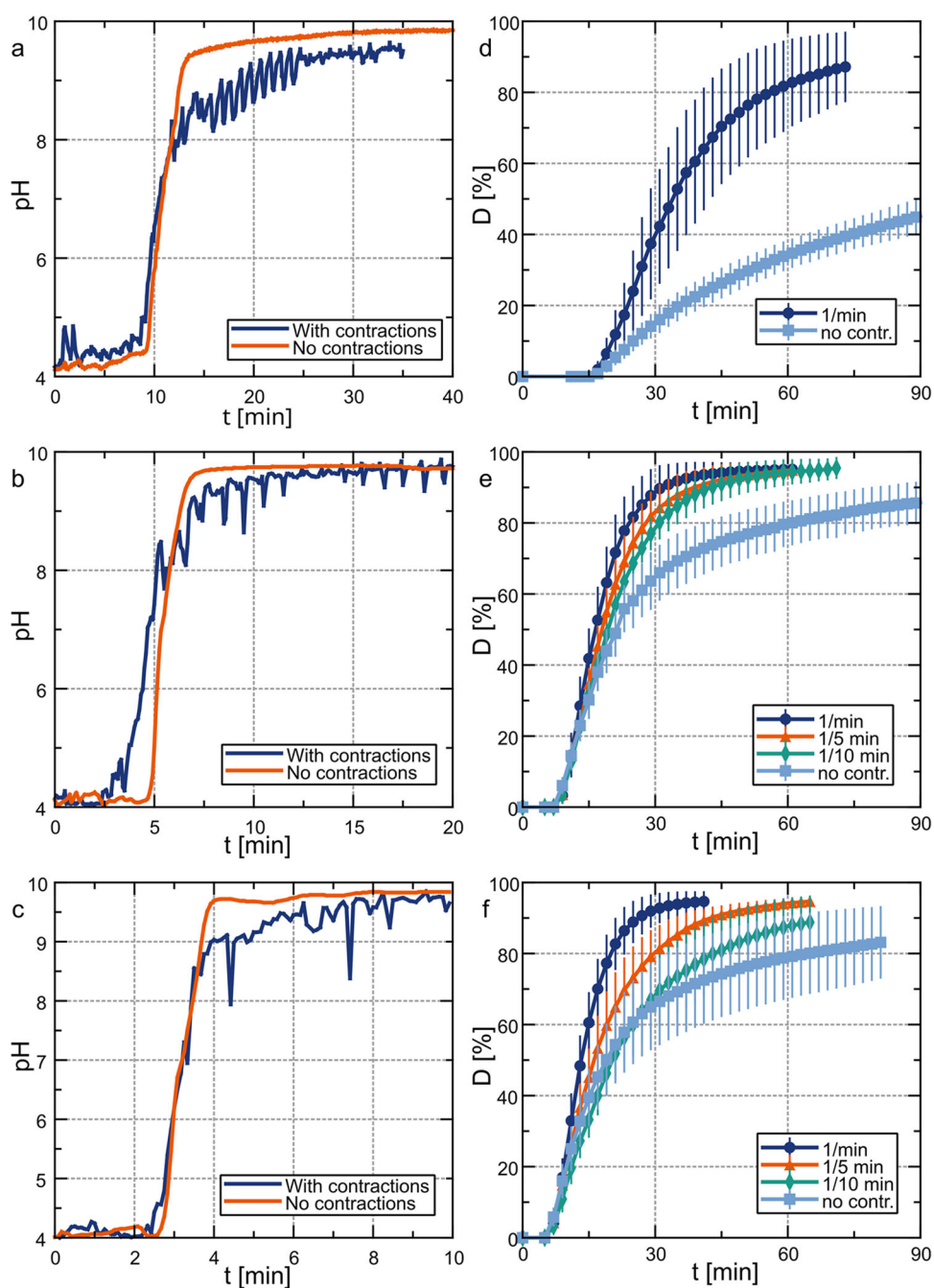
**Table IV**  $T_{85}$  for the Paracetamol Under Various Flow Rates and Frequencies of Mixing Contractions

Flow rate [mL/min]	Frequency of the mixing contractions			
	1/min	1/5min	1/10min	none
4	67	—	—	—
8	27	33	37	85
12	23	35	53	—

the compendial USP 4 flow-through apparatus. Hence, the hydrodynamics of the two systems should be similar. Simple visual observations of the flow pattern reported

in this study lack the sophistication and complexity of the computer-aided simulations. However, they are a good tool for monitoring strong local fluctuations in the system.

**Fig. 7** Influence of contractions on the pH gradient formation recorded in the proximity of outlet tube of the StressCell under various flow rates: **a** medium flow 4 mL/min, **b** medium flow 8 mL/min, and **c** medium flow 12 mL/min. Influence of contraction frequencies of the StressCell's elastic sleeve on paracetamol tablet dissolution: **d** medium flow 4 mL/min, **e** medium flow 8 mL/min, and **f** medium flow 12 mL/min



Initially, we observed how the medium flows in the *StressCell*. Through visual assessment of the  $\text{KMnO}_4$  solution, we noticed a parabolic shape of the flow profile at 8 mL/min. This observation resembles investigations of the compendial USP 4 apparatus. Shiko et al. [23] studied USP 4 flow patterns with magnetic resonance imaging. They also observed jetty flow with an almost parabolic profile at 8 and 16 mL/min rates. Of note, the internal diameter of USP 4 was similar to the *StressCell*: 22.6 mm vs. 24.2 mm, respectively. The difference from our experiment was a recirculation zone in the proximity of the cell's wall. The authors associated the recirculation with a temperature gradient near the wall. In the *PhysioCell* experiment, the dissolution medium and the *StressCell* were kept at room temperature. Therefore, such zones were not present.

As in the USP 4, the formulation in the *StressCell* lies on a glass bead layer. We observed that neither the layer's thickness, nor the bead size significantly affected the dissolution rate, except for the smallest beads. Most probably, the peristaltic pump caused a non-continuous medium flow that increased the movement of the beads. Then, it led to the *NaCl* tablet sinking and increased erosion of its surface. Our observations are consistent with the compendial flow-through apparatus. Eaton et al. evaluated the impact of the number and size of glass beads on the dissolution of salicylic acid tablets in USP 4 [24]. The authors concluded that the diameter of glass beads was the most crucial parameter impacting the dissolution rate and its variability, not their number. An important note is that we did not examine the dissolution for the most widely used 1 mm glass beads extensively. However, in other experiments, we noticed that such beads sufficiently support the dosage form (data not reported). Therefore, we expect the dissolution to be comparable with the 2 mm glass beads.

In the present study, we observed that the dissolution rate of two tested tablets (*NaCl* and *Strepsils*<sup>®</sup>) was not proportional to the flow rate. Such observations in flow-through apparatuses were made by other researchers [25, 26]. We expected that a reduction of the flow rate would decrease the dissolution rate, since under conditions of low medium flow, the diffusion would be the main mechanism of the transport of the dissolved API. Then the thickness of the diffusion layer would be the largest and the dissolution the slowest. Surprisingly, we noticed that with the flow of 4.6 mL/min the observed dissolution time of *NaCl* was shorter (16.0 min) than with the flow 9.0 mL/min (17.5 min). Therefore we suppose that, at the low flow rates, not only the diffusion influences the dissolution rate. The hydrodynamic conditions in proximity of a dosage form are influenced by gravitational force that causes the dense dissolved material to flow down the dissolution chamber, against the medium which is pumped upward, leading to the dissolution acceleration. This hypothesis is supported by the observation of a

stream of dissolved substance moving downwards the cell (Fig. 2). Therefore, at the low flow rates, the free convection becomes the primary mechanism driving the dissolution in the *StressCell*. It has been shown that the slow (up to 6 mL/min) upward stream of the medium in a USP4 apparatus does not penetrate into the natural convection-formed concentration boundary layer, but only flows around it [29]. In the cited work, when the upward flow in the large flow-through cell increased up to 8 mL/min, the natural and forced convection interfered, the downward migration of the dissolved molecules slowed down, and the dissolution rate reached the minimum. The upward medium flow and free convection are counter-productive processes during the dissolution. This phenomenon most likely occurs also in the *StressCell*, and accounts for the slower dissolution of *NaCl* at the flow rate 9.0 than at 4.6 mL/min. The observations from the reverse-flow experiments support the hypothesis about the free convection governing the dissolution of *NaCl* — a highly soluble compound. We observed a higher dissolution rate of the substance when the medium was pumped from the top to the bottom of the *StressCell*. At such conditions, the applied downward medium flow enhances the molecules' downward motion due to free convection, leading to the increased dissolution rate. The impact of the dissolved substance on the local hydrodynamic conditions and dissolution rate is dependent on the API solubility and density of its solution [27]. Highly soluble substances of large molecular weight can produce a dense solution in its proximity and the difference of densities between such a solution and pure dissolution medium can result in convective mass transfer; thus influencing the hydrodynamics around the dissolving dosage form. Such a mechanism was proposed by D'Arcy et al. [30]. The authors utilized Computational Fluid Dynamics simulations to characterize the dissolution of benzoic acid and lactose monohydrate. In their study, a system with no agitation provided better mass transfer than a flow-through apparatus with medium flowing counter-gravity. On the other hand APIs of low solubility are expected to undergo this mechanism only to a limited extent [27] and their dissolution should be the slowest under conditions of no medium flow. Stevens and Missel observed no effect of the medium flow direction on the dissolution of poorly soluble anecortave acetate in contrast to moderately-soluble benzocaine [28]. It stems from a much lower saturation concentration in the boundary layer and negligible density gradients [28, 29]. Also, D'Arcy et al. expect similar density effects to occur *in vivo*, especially in conditions of low medium volume and limited agitation. However, from a physiological point of view, the absolute lack of movement is unlikely to appear in the GI tract. For example, a delicate diaphragm motion during breathing influences other organs in the abdomen. Thus we introduced

delicate mixing contractions of the elastic sleeve, building the wall of the *StressCell*.

With the flow rate increase, free convection's importance decreases. Similar dissolution profiles of *NaCl* tablets at a flow of 42–86 mL/min and *Strepsils*<sup>®</sup> at 44 and 81 mL/min may signalize an increase of forced convection contribution in the dissolution. Flow rates within 80–180 mL/min enhanced the dissolution by decreasing the  $T_{85}$  time by ca. 40%; rates greater than 180 mL/min did not seem to have any effect on the dissolution rate of *NaCl*, since the  $T_{85}$  remained equal to 6 min. Also, the function fitted to dissolution time of *NaCl* tablets vs. flow rate has a finite value even at theoretical infinite flow rate. With very high flow rate, the dissolved substance is carried out by the flowing medium, and gravity's effect is insignificant. But another mechanism is responsible for limiting the dissolution: the transfer of the dissolving substance between the dosage form and the boundary layer. If this transfer is slow, it becomes a limiting step, and even very high flow rates will not increase the overall dissolution rate. The idea of only limited ability of a system to supply drug to the boundary layer and maintain the saturation solubility therein was presented by Missel et al. [31]. Also, Sleziona et al. [32] described the drug release as a process consisting of a surface reaction and diffusion: in the first step (the surface reaction) a solid API dissolves to the liquid phase and then diffuses through the diffusion layer into the bulk medium. Each of these steps can limit the dissolution rate, which is in accordance with our results.

What differentiates the *StressCell* from the compendial flow-through apparatus is an elastic sleeve that enhances the mixing of the *StressCell* contents. First, we observed that the contractions altered how the medium flowed and exchanged inside the chamber. Instead of a piston-like flow followed by an almost instantaneous pH shift, the contractions caused a more gradual exchange with noticeable fluctuations. Of note, during these experiments with buffers, pH was assessed only locally in a single point of the cell. Therefore, these results do not give a complete view of the pH distribution in the whole *StressCell* volume and point at the complexity of the mixing processes. Next, the experiments with rapidly disintegrating paracetamol tablets showed that various frequencies of the contractions influenced the dissolution rate, especially at low flow rates that correspond to the low gastric emptying kinetics of water. For example, introduction of the mixing contractions with a frequency of 1 per 10 min at the flow rate of 8 mL/min resulted in over 2-fold decrease of the  $T_{85}$  and further increase of the frequency to 1 per minute decreased the  $T_{85}$  over 3 times. Dissolution medium flow rates of 4, 8 and 12 mL/min we tested are aligned with values of gastric emptying under fasted conditions determined with Echo-Planar and Magnetic Resonance Imaging [33–35].

Typically, 240 mL of non-caloric, low viscous liquid is emptied in 45 min with almost exponential kinetics and half time 13 min, which corresponds to an average value of 9.3 mL/min in the first half of the process and total mean value of 5.4 mL/min [34]. We also tested dissolution under higher flow rates to broaden our understanding of processes occurring in the apparatus.

The contractions of the sleeve may help the dissolution medium to penetrate the previously mentioned downflow of dissolved substance and to ruffle a cone of the disintegrated dosage form. Also, for low medium flow rate and without mixing, sink conditions are questionable since the dense dissolved matter has difficulties evacuating from the cell efficiently. On a molecular level, the mixing contractions are expected to aid the transfer of the dissolved substance from the boundary layer to the medium bulk and provide the boundary layer with fresh dissolution medium. Thus, they serve as an additional convective transfer of the dissolved substance. The obtained results prove that even mild mechanical agitation affects the dissolution process.

While this report describes the hydrodynamics and mixing conditions as the most important aspects of the *PhysioCell*, several issues have to be addressed in future experiments. For instance, mechanical agitation during the gastrointestinal passage has various intensities and frequencies of contractions. In the present report, we focused on the frequency of the mixing contractions and a detailed dissolution analysis under varying pressure events applied directly on a dosage form were outside the scope. In further experiments, the capability of the *PhysioCell* to realistically mimic the motility patterns and fortitude of physiological pressure events will be investigated along with the dissolution performance of model dosage forms. Utilizing the feature of the pressure wave application, the *PhysioCell* enables the simulation of the housekeeper wave that appears during the gastric emptying in the third phase of the migrating motor complex under fasted conditions. This is achieved by a series of pressure waves that help to transport the content of the *StressCell* to the *Overflow Vessel*. The GE sequence time can be adjusted in the test scenario, which means that not only one, but a series of test protocols can be incorporated into the testing of a formulation, thus reflecting a variable GE time, as it occurs *in vivo* [22, 36]. Therefore the *PhysioCell* offers a possibility to test a dosage form under conditions of varying gastric transit time. Such an approach was also found valuable in the other bio-relevant apparatus, the GastroDuo [17]. The next factor that requires a detailed investigation is the simulation of physiological gradients of temperature. Although enabled by the setup, the detailed description of the simulation procedure will be the aim of subsequent studies. In the present work, we only roughly demonstrated the pH shift in the *StressCell*. However, the construction of

the device, especially its *Overflow Vessel*, allows to perform rapid neutralization of the simulated gastric media. This challenging aspect requires further investigations and will be described separately.

The next challenge to overcome is understanding how natural convection and mild mixing control dissolution *in vivo*. Physiologically, the intestinal conditions comprise the flow counter the gravitation [37], low fluid volumes present as small pockets [38] and mixing by peristaltic movements. Therefore, all these effects need to be incorporated to most closely capture the *in vivo* conditions. Lastly, the reported experiments utilized only the StressCell and well-soluble substances. Thus, the dissolution in the near-sink setting, for poorly soluble compounds and with utilization of the neutralization module of the Overflow Vessel and Collection Vessel is yet to be examined.

Moreover, despite plenty of beneficial features, *PhysioCell* itself bears some limitations. Firstly, simulating fed conditions or utilizing complex dissolution media like digested milk or food, might be challenging due to the narrow tubing of the device. Secondly, dissolution tests of extended release dosage forms would require further adjustment of the experimental setup and test protocols. Also, for now, no absorption compartment is included in the construction of the apparatus. *PhysioCell* is designed for conditions of the stomach and small intestine; thus simulation of colonic conditions is limited to the application of enzymes and physiological pH and the apparatus is unsuitable for the cultivation of bacteria cultures. Finally, some APIs may interact with materials of the construction (e.g., latex, silicone, PCV) and preliminary experiments would be required to assess it.

## Conclusions

In summary, the preliminary experiments presented in this work allowed to detect the features of the novel apparatus that influence the dissolution process: the medium flow rate and the physiological mixing contractions. The flow rate was found to nonlinearly increase the dissolution rate and the introduction of mixing contractions decreased the dissolution time. Along with the capability of simulating the GI pressure waves, pH fluctuations, and temperature gradients, these features will allow the *PhysioCell* to become a powerful tool for creating bio-relevant conditions *in vitro* that closely resemble the dissolution *in vivo*.

**Supplementary Information** The online version contains supplementary material available at <https://doi.org/10.1208/s12249-022-02494-4>.

**Acknowledgements** The authors would like to kindly thank Prof. Sebastian Polak, PhD Grzegorz Banach and PhD Jadwiga Paszkowska for critically reviewing the final version of the manuscript.

**Author Contribution** Conceptualization: Marcela Staniszevska, Grzegorz Garbacz. Methodology: Marcela Staniszevska, Justyna Dobosz, Bartosz Kołodziej, Uladzimir Lipski. Formal analysis and investigation: Marcela Staniszevska, Grzegorz Garbacz. Writing — original draft preparation: Marcela Staniszevska, Dorota Danielak. Writing — review and editing: Michał; Romański, Grzegorz Garbacz. Funding acquisition: Grzegorz Garbacz. Supervision: Dorota Danielak, Grzegorz Garbacz.

**Funding** The work has been partially financed by Polish National Centre for Research and Development (POIR.01.02.00-00-0011/17).

## Declarations

**Conflict of Interest** The authors declare no competing interests.

## References

- Garbacz G, Rappen GM, Koziolok M, Weitschies W. Dissolution of mesalazine modified release tablets under standard and bio-relevant test conditions. *J Pharm Pharm*. 2015;67(2):199–208.
- Fadda HM, Merchant HA, Arafat BT, Basit AW. Physiological bicarbonate buffers: stabilisation and use as dissolution media for modified release systems. *Int J Pharm*. 2009;382(1-2):56–60.
- Jantratid E, De Maio V, Ronda E, Mattavelli V, Vertzoni M, Dressman JB. Application of biorelevant dissolution tests to the prediction of *in vivo* performance of diclofenac sodium from an oral modified-release pellet dosage form. *Eur J Pharm Sci*. 2009;37(3-4):434–441.
- Schiller C, Fröhlich CP, Giessmann T, Siegmund W, Mönikes H, Hosten N, et al. Intestinal fluid volumes and transit of dosage forms as assessed by magnetic resonance imaging. *Alimentary Pharmacology & Therapeutics*. 2005;22:971–979.
- Schneider F, Grimm M, Koziolok M, Modeß C, Dokter A, Roustom T, et al. Resolving the physiological conditions in bioavailability and bioequivalence studies: Comparison of fasted and fed state. *Eur J Pharm Biopharm*. 2016;108:214–219.
- Garbacz G, Cadé D, Benameur H, Weitschies W. Bio-relevant dissolution testing of hard capsules prepared from different shell materials using the dynamic open flow through test apparatus. *European J Pharm Sci*. 2014;57:264–272.
- Jede C, Wagner C, Kubas H, Weigandt M, Weber C, Lecomte M, et al. Improved prediction of *in vivo* supersaturation and precipitation of poorly soluble weakly basic drugs using a biorelevant bicarbonate buffer in a gastrointestinal transfer model. *Molecular Pharmaceutics*. 2019;16(9):3938–3947.
- Garbacz G, Wedemeyer RS, Nagel S, Giessmann T, Mönikes H, Wilson CG, et al. Irregular absorption profiles observed from diclofenac extended release tablets can be predicted using a dissolution test apparatus that mimics *in vivo* physical stresses. *European Journal of Pharmaceutics and Biopharmaceutics*. 2008;70:421–428.
- Diebold S. Physiological parameters relevant to dissolution testing: hydrodynamic considerations. Taylor & Francis: London UK. 2005.
- Abrahamsson A, Pal M, Sjöberg M, Carlsson E, Laurell JGB. A novel *in vitro* and numerical analysis of shear-induced drug release from extended-release tablets in the fed stomach. *Pharmaceutical Research*. 2005;22(8):1215–1226.
- Wiater M, Hoc D, Paszkowska J, Garbacz G. Hydrodynamics and mechanical stresses in pharmacopoeial and noncompendial dissolution testing. *Farmacja Polska*. 2020;76(4):210–221.

12. McAllister M. Dynamic dissolution: a step closer to predictive dissolution testing?. *Molecular Pharmaceutics*. 2010;7(5):1374–1387.
13. Minekus M. The TNO gastro-intestinal model (TIM). Cham: Springer; 2015, pp. 37–46.
14. Hribar M, Trontelj J, Berglez S, Bevc A, Kuscer L, Diaci J, et al. Design of an innovative advanced gastric simulator. *Dissolution Technologies*, 20–29. 2019.
15. Wickham MSJ, Faulks RM, Mann J, Mandalari G. The design, operation, and application of a dynamic gastric model. *Dissolution Technologies*. 2012;19(3):15–22.
16. Kourentas A, Vertzoni M, Stavrinoudakis N, Symillidis A, Brouwers J, Augustijns P, et al. An in vitro biorelevant gastrointestinal transfer (BioGIT) system for forecasting concentrations in the fasted upper small intestine: design, implementation, and evaluation. *European Journal of Pharmaceutical Sciences*. 2016;82:106–114.
17. Schick P, Sager M, Wegner F, Wiedmann M, Schapperer E, Weitschies W, et al. Application of the GastroDuo as an in vitro dissolution tool to simulate the gastric emptying of the post-prandial stomach. *Molecular Pharmaceutics*. 2019;16(11):4651–4660.
18. Li Y, Kong F. Simulating human gastrointestinal motility in dynamic in vitro models. *Compr Rev Food Sci Food Safety*. 2022;21(5):3804–3833.
19. Wilson C, Aarons L, Augustijns P, Brouwers J, Darwich A, De Waal T, et al. Integration of advanced methods and models to study drug absorption and related processes: An UNGAP perspective. *European Journal of Pharmaceutical Sciences*, 106100. 2021.
20. Staniszevska M, Kolodziej B, Paszkowska J, Dobosz J, Garbacz G, Banach G. A flow-through cell for testing the behavior of a pharmaceutical dosage form, the system containing it and the method of homogenizing the dissolution medium P43946. 2021.
21. Koziolok M, Schneider F, Grimm M, Modess C, Seekamp A, Roustom T, et al. Intra-gastric pH and pressure profiles after intake of the high-caloric, high-fat meal as used for food effect studies. *J Controlled Release*. 2015;220:71–78.
22. Koziolok M, Grimm M, Becker D. Investigation of pH and Temperature Profiles in the GI Tract of Fasted Human Subjects Using the Intellicap System. *Pharmaceutics, Drug Del Pharm Technol*. 2014;104:2855–2863.
23. Shiko G, Gladden L, Sederman A, Connolly P, Butler J. MRI studies of the hydrodynamics in a USP 4 dissolution testing cell. *J Pharmaceutical Sci*. 2011;100(3):976–991.
24. Eaton JW, Tran D, Hauck WW, Stippler ES. Development of a performance verification test for USP apparatus 4. *Pharmaceutical Research*. 2012;29(2):345–351.
25. Krämer J, Stippler E. Experiences with USP apparatus 4 calibration. *Dissolution Technol*. 2005;12(2):33–39.
26. Fang J, Robertson V, Rawat A, Flick T, Tang Z, Cauchon N, et al. Development and application of a biorelevant dissolution method using USP apparatus 4 in early phase formulation development. *Molecular Pharmaceutics*. 2010;7(5):1466–1477.
27. D’Arcy D, Corrigan O, Healy AM. Evaluation of hydrodynamics in the basket dissolution apparatus using computational fluid dynamics—dissolution rate implications. *European J Pharmaceutical Sci*. 2006;27(2-3):259–267.
28. Stevens L, Missel P. Impact of density gradients on flow-through dissolution in a cylindrical flow cell. *Pharm Dev Technol*. 2006;11(4):529–534.
29. McDonnell D, D’Arcy D, Crane L, Redmond B. A mathematical analysis of drug dissolution in the USP flow through apparatus. *Heat and Mass Transfer*. 2018;54(3):793–801.
30. D’Arcy D, Liu B, Corrigan O. Investigating the effect of solubility and density gradients on local hydrodynamics and drug dissolution in the USP 4 dissolution apparatus. *Int J Pharm*. 2011;419(1-2):175–185.
31. Missel PJ, Stevens LE, Mauger JW. Reexamination of convective diffusion/drug dissolution in a laminar flow channel: accurate prediction of dissolution rate. *Pharm Res*. 2004;21(12):2300–2306.
32. Sleziona D, Mattusch A, Schaldach G, Ely DR, Sadowski G, Thommes M. Determination of inherent dissolution performance of drug substances. *Pharmaceutics*. 2021;13(2):146.
33. Marciani L, Gowland PA, Spiller RC, Manoj P, Moore RJ, Young P, et al. Effect of meal viscosity and nutrients on satiety, intragastric dilution, and emptying assessed by MRI. *Am J Physiol-Gastrointestinal Liver Physiol*. 2001;280(6):G1227–G1233.
34. Mudie DM, Murray K, Hoad CL, Pritchard SE, Garnett MC, Amidon GL, et al. Quantification of gastrointestinal liquid volumes and distribution following a 240 mL dose of water in the fasted state. *Mol Pharmaceutics*. 2014;11(9):3039–3047.
35. Steingoetter A, Fox M, Treier R, Weishaupt D, Marincek B, Boesiger P, et al. Effects of posture on the physiology of gastric emptying: a magnetic resonance imaging study. *Scand J Gastroenterol*. 2006;41(10):1155–1164.
36. Goyal RK, Guo Y, Mashimo H. Advances in the physiology of gastric emptying. *Neurogastroenterology & Motility*. 2019;31(4):e13546.
37. Weitschies W, Blume H, Mönnikes H. Magnetic marker monitoring: high resolution real-time tracking of oral solid dosage forms in the gastrointestinal tract. *Eur J Pharm Biopharm*. 2010;74(1):93–101.
38. Schiller C, Fröhlich CP, Giessmann T, Siegmund W, Mönnikes H, Hosten N, et al. Intestinal fluid volumes and transit of dosage forms as assessed by magnetic resonance imaging. *Aliment Pharmacol Ther*. 2005;22(10):971–979.

**Publisher’s Note** Springer Nature remains neutral with regard to jurisdictional claims in published maps and institutional affiliations.

Springer Nature or its licensor (e.g. a society or other partner) holds exclusive rights to this article under a publishing agreement with the author(s) or other rightsholder(s); author self-archiving of the accepted manuscript version of this article is solely governed by the terms of such publishing agreement and applicable law.